Am J Transl Res 2023;15(3):2191-2206
www.ajtr.org /ISSN:1943-8141/AJTR0148287

Original Article

COX10-AS1-mediated miR-361-5p regulated cell invasion and migration by targeting SPRY1 in oral squamous cell carcinoma

Jing Deng[1*], Maolin Wu[2*]

[1]*Department of Otolaryngology, Hospital of Chengdu University of Traditional Chinese Medicine, Chengdu 610075, Sichuan, China;* [2]*Department of Oncology, Hospital of Chengdu University of Traditional Chinese Medicine, Chengdu 610075, Sichuan, China.* [*]*Equal contributors.*

Received December 7, 2022; Accepted February 2, 2023; Epub March 15, 2023; Published March 30, 2023

Abstract: Background: COX10-AS1 belongs to the class of lncRNA and has been shown to influence carcinogenesis; however, its function and underlying mechanism in oral squamous cell carcinoma are still unclear (OSCC). Method: Western blotting, immunohistochemistry, and RT-PCR were used to identify gene expression. Cell invasion and migration were discovered using Transwell and Scratch-Wound analyses. The interaction between lncRNA and miRNA was examined using dual-luciferase and immunofluorescence assays. Results: We discovered that COX10-AS1 was significantly downregulated in OSCC tissues when compared to matched noncancerous tissues, indicating a dismal prognosis for OSCC patients. By raising the expression of MMP-2/-9 and Snail and lowering the expression of E-cadherin, COX10-AS1 deletion increased OSCC cell invasion and migration. Next, three binding sites between COX10-AS1 and miR-361-5p were shown in the StarBase V2.0 database. Pearson's correlation analysis revealed a negative association between the expression of COX10-AS1 and that of miR-361-5p, and miR-361-5p transfection reduced COX10-AS1's influence on OSCC cell invasion and migration. Furthermore, COX10-AS1 favorably regulated SPRY1, a miR-361-5p target gene. Conclusion: Through the miR-361-5p/SPRY1 axis, COX10-AS1 can act as a tumor suppressor and is decreased in OSCC.

Keywords: COX10-AS1, OSCC, miR-361-5p, migration, invasion

Introduction

Oral squamous cell carcinoma (OSCC) ranks as the sixth most common malignancy with increasing morbidity and mortality [1]. In China, approximately 48,100 new-onset OSCC cases and 22,100 deaths have occurred annually [2, 3]. Smoking, alcohol or areca abuse are the main risk factors for the disease and local recurrence and distant metastasis mainly obstruct the OSCC treatment [4]. Despite the development of treatment, the survival for OSCC patients remains unsatisfactory, and the metastasis and recurrence are the most deteriorated factors of prognosis. Identifying efficient biomarkers and mechanisms related to OSCC recurrence and metastasis is imperative.

Long non-coding RNAs (lncRNAs), without an open reading frame (ORF), are a type of non-coding RNA with over 200 nucleotides in length [5]. Accumulating evidence has demonstrated that the dysregulation of lncRNAs can participate in the initiation and progression of various cancers via regulating cell proliferation, apoptosis, differentiation, and carcinogenesis. LINC01793 has been reported as a poor prognostic biomarker of OSCC [6], and ZEB1-AS1, LHFPL3-AS1, and DLEU1 act as oncogenes in OSCC [7-9]. LncRNA CCAT2 is highly expressed in colorectal cancer tumor tissues [10], osteosarcoma tissues [11], and glioma [12] to promote cell proliferation and migration and has poor prognosis. Downregulation of LINC-PINT in multiple types of cancer acts as a tumor suppressor [13]. However, lncRNA H19 is a typical example that can function either as a tumor promoter or a tumor suppressor [14]. These results indicate that the same lncRNA can be expressed in the same or different ways in dif-

ferent tumors to play a pro-cancer or anti-cancer role, while different lncRNAs play different roles in tumors. In this study, COX10-AS1, is a non-coding transcript located on chromosome 17, and its role in cancer is quite limited. COX10-AS1 has only been reported in its overexpression inducing ACTG1-increase to accelerate tumorigenesis in glioblastoma, also clarifying that low expression of COX10-AS1 was associated with low survival possibility in triple-negative (TN) breast cancer [15, 16]. We hypothesized that COX10-AS1 might be another lncRNA that can function either in a pro-cancer or an anti-cancer fashion. COX10-AS1 was reported to significantly downregulate in OSCC patients [17]. Therefore, we investigated the role of this lncRNA in OSCC and preliminarily explored its mechanism.

MicroRNAs, also known as miRNAs, are short molecules of non-coding RNA that contain around 22 nucleotides and are responsible for regulating gene expression by inhibiting or promoting the degradation of target messenger RNAs [18]. They have a role in a wide variety of biological processes, such as the differentiation and proliferation of cells, the metabolism, and the apoptosis of cells. Since the structure of the majority of lncRNAs is comparable to that of mRNA to some extent, this suggests that the expression of lncRNAs may be negatively regulated by miRNAs through a mechanism that is comparable to the mechanism by which miRNA regulates mRNA, and as a result, they play a variety of important roles in biological processes [19]. LncRNAs compete with miRNA for binding sites on the 3'-untranslated region (UTR) of target gene mRNA, which results in an indirect inhibition of the negative regulation of target genes by miRNA [20]. Additionally, lncRNAs have the potential to act as endogenous miRNA sponges and suppress the production of miRNAs [21]. As a result, an integrated study of the regulatory interaction between miRNA, lncRNA, and mRNA is capable of providing a more thorough explanation for the onset and progression of OSCC.

Materials and methods

Clinical specimens

The Ethics Committee of the Hospital affiliated with Chengdu University of Traditional Chinese Medicine gave its approval to proceed with this investigation. Between June 1, 2015 and December 30, 2020, individuals with OSCC provided samples of their tumor tissues as well as surrounding normal tissues to match. Every patient signed the consent form.

Immunohistochemistry (IHC)

The immunohistochemistry was carried out via a kit (Beyotime) in accordance with the instructions provided by the manufacturer. In a nutshell, tissue was regularly deparaffinized and rehydrated sections were embedded in paraffin at a thickness of 4 micrometers. The sections were microwaved in a citrate solution with 10 mM concentration to retrieve the antigens. The use of 3% hydrogen peroxide was used to inhibit the activity of endogenous peroxidase. After that, the slides were left at room temperature for twenty minutes while they were incubated with a standard goat serum seal solution. After that, the slides were incubated with primary antibodies directed against SPRY1 at a temperature of 4 degrees Celsius for the duration of one full night. After that, the slides were incubated with biotin-labeled goat anti-mouse/rabbit IgG secondary antibodies at room temperature for ten minutes. The streptavidin-peroxidase mixture was left to sit at room temperature for 15 minutes before being developed with DAB. After that, the sections were counterstained for two minutes. After that, the sections were preserved by drying them out and then sealing them with neutral gum. PBS was utilized as the main antibody replacement for the purpose of the negative control. The results were graded twice, once using a qualitative scale and once using a quantitative scale.

Cell culture and transfection

Cells from the OSCC cell lines (HSC-4, SCC-25, CAL27, and CAL33) as well as the human oral squamous cell carcinoma cell line CAL-27 were received from the Cell Bank (Shanghai, China). The cell line CAL-27 was grown in Dulbecco's modified Eagle's medium (DMEM) supplemented with 10% fetal bovine serum (FBS). OSCC cell lines were grown in DMEM/F12 with 10% fetal bovine serum at 37 degrees Celsius and 5% carbon dioxide (FBS; all from Gibco, Grand Island, NY, USA). Genepharma was responsible for the synthesis of two small interfering RNAs (siRNAs) to COX10-AS1 (si-COX10-AS1#1 and #2), a control siRNA (siNC), the pcDNA3.1 over-

Table 1. The sequences of the primers

Gene	Forward (5'-3')	Reverse (5'-3')
COX10-AS1	AGGAAAGATGCACCCCTGTA	GTAACTCCCACAATTCCCACA
miR-361-5p	ATAAAGTGCTGACAGTGCAGATAGTG	TCAAGTACCCACAGTGCGGT
SPRY1	AGCAGTAGGTAGTTGTGGGA	AGCCATCTCTTCCGCTGATT
U6	CTCGCTTCGGCAGCAGCACATATA	AAATATGGAACGCTTCACGA
GAPDH	ACCTTAACCGCCTTATTAGCCA	CACCACGGTACAACAGGCA

expressing vector (COX10-AS1), a control vector (vector), mimics, inhibitors, and NC of miR-361-5p (Shanghai, China). After that, 1 × 10^6 OSCC cells were transfected with 2 g of pcDNA3.1-COX10-AS1 or siRNAs, mimics, or inhibitors using Lipofectamine 3000 (Thermo Fisher Scientific, Waltham, MA, USA). Gene expression was measured after 48 hours of culture. Last but not least, OSCC was co-transfected with either miR-361-5p mimics and COX10-AS1 or miR-361-5p inhibitors and si-COX10-AS1 to see which combination produced the best results. In preparation for further tests, the cells were cultivated for a total of 48 hours. The target sequence of human COX10-AS1#1 silencing is GTAGGCCAACTC-TCACATA and the target sequence of human COX10-AS1#2 silencing is ATGGTGTCGTGC-CATGTGAA.

Quantitative real-time PCR (RT-PCR)

First, total RNA from tissues and cells was extracted using RNeasy kits (Qiagen, Valencia, California, USA), and then the PrimeScript RT Kit was used to do reverse transcription, which resulted in cDNA (Takara, Dalian, China). SYBR-Green was utilized for the quantitative PCR, which was carried out using the StepOnePlus Real-Time PCR System (Applied Biosystems, CA, USA) (Takara). The following were the terms and conditions: 95 degrees Celsius for five minutes, then 40 cycles of 95 degrees Celsius for 15 seconds and 58 degrees Celsius for forty minutes each. The GAPDH and U6 genes were employed as an internal reference, and the 2-Ct technique was applied to determine the level of expression. **Table 1** contains a listing of the primers that were utilized.

Wound healing assay

On order to generate wounds, two replicates of 105 cells were grown in 6-well plates until they reached 100% confluence, and then a scratch was formed using a 10-ul tip. After being washed twice with PBS, the cells were cultured for a further 24 hours in media that did not include any serum. Under an Olympus microscope with a magnification of 100, images of the wounds were captured, and the surface area of the scratch was determined.

Transwell assay

The cells were seeded into the upper chamber of the transwell chamber (BD Pharmingen) with or without pre-coated Matrigel (BD Pharmingen) while the lower chamber was filled with medium supplemented with 20% FBS. The cells were suspended in 100 ul of DMEM without FBS and then seeded into the upper chamber of the transwell chamber. The migrating or invasive cells were stained with a crystal violet solution (Beyotime, Nanjing, China) at 37 degrees Celsius for ten minutes after being fixed with 4% methanol at 37 degrees Celsius for thirty minutes. Under an Olympus microscope with a magnification of 200, the cells were evaluated and measured for size.

Dual-luciferase reporter assay

The 3'-untranslated sections of COX10-AS1 and SPRY1 that contain wild-type (wt) or mutant (mut) binding sites for miR-361-5p were amplified and introduced into the psiCHECK2 vector in order to construct wt-COX10-AS1/SPRY1 and mut-COX10-AS1/SPRY1 plasmids, respectively. This was done in order to construct wt-COX10-AS1/(Promega, WI, USA). Co-transfection of wild-type or mutant COX10-AS1/SPRY1 vectors with miR-361-5p mimics/inhibitors or with negative control molecules was accomplished with the assistance of Lipofectamine 3000 (Thermo Fisher Scientific). After 48 hours of culture, luciferase activity was measured with a Dual-Luciferase Reporter Assay System. This was done after the culture had been in place (Promega).

Immunofluorescence assay

OSCC cells were fixed using pre-chilled paraformaldehyde at a concentration of 4% (PFA,

Beyotime, Shanghai, China). The cells were then washed three times with PBS, permeabilized with PBS that included 0.1% Triton X-100, and then washed three times with PBS that contained 0.05% Tween 20. After the samples were blocked for an hour at room temperature with PBS containing 3% bovine serum albumin (BSA), they were taken for analysis. Antibodies directed against SPRY1 were diluted to a 1:2,000 ratio and purchased from Abcam in Cambridge, Massachusetts, and were incubated with the cells at room temperature for one hour. After being washed, the cells were treated with DAPI and an Alexa-Fluor-488-conjugated anti-rabbit-IgG antibody for the purpose of SPRY1 detection (1:1,000, InvitrogenTM; Thermo Fisher Scientific). Fluorescence microscopy using a Zeiss Axio Imager Z1 was used to image the specimens after they were mounted (Zeiss, Germany).

In situ hybridization (ISH)

The *in situ* hybridization (ISH) was carried out utilizing a kit (supplied by Shanghai Gefan Biotechnology co., LTD., China) in accordance with the instructions provided by the manufacturer. In a nutshell, an *in situ* hybridization probe that is specific for COX10-AS1 was created, and Boster bioengineering co., LTD. was responsible for the synthesis of the probe (Boster, Wuhan, China). At room temperature for two minutes, paraffin-embedded OSCC and matched neighboring tissue slices were digested with pepsin that had been diluted with fresh citrate at a concentration of 3%. After that, the sections were deparaffinized and rehydrated, rinsed with PBS three times for five minutes, then washed with distilled water, and last, they were incubated at 37 degrees Celsius for two hours with twenty microliters of preliminary hybrid liquid. After that, the slides were further subjected to an overnight incubation at a temperature of 42 degrees Celsius with 20 microliters of hybrid liquid. As part of the negative control experiment, the hybrid liquid used in the experiment was switched out for a preliminary hybrid liquid. After the hybridization step, the slides were first washed with gradient dilution solution buffer, then they were incubated with biotin-labeled rat anti-digoxin for an hour and a half at 37 degrees Celsius, and finally they were rinsed with PBS four times. Each slide was had DAB development, and further examination was carried out using an optical microscope. After being counterstained with Mayer's Hematoxylin and distinguished with 0.1% alcohol hydrochloride, tissues were rinsed in running water to remove any residual staining. The slides were then subjected to a process of dehydration before being sealed with neutral gum. The fluorescent microscope (model BX-51TRF, manufactured by OLYMPUS in Japan) was used to take images, and a favorable result was denoted by a brown color. The results were graded twice, once using a qualitative scale and once using a quantitative scale.

Western blot assay

RIPA buffer (Beyotime) was used to lyse the cells, and then the BCA kit was used to determine the amount of protein present (ThermoFisher). Through 12% SDS-PAGE analysis, equal amounts of protein were separated, and then those separated proteins were put to an Immobilon-P membrane (Millipore, MA, USA). After blocking the membrane with a solution containing 5% skim milk for two hours, the membrane was subjected to an overnight incubation at 4 degrees Celsius with the following primary antibodies: rabbit anti-SPRY1 (1:1000, ab111523 from Abcam, UK), and rabbit anti-GAPDH (1:5000, ab9485, Abcam). Abcam served as the source for all of the antibodies. After that, an HRP-conjugated goat anti-rabbit IgG secondary antibody (ab205718; Abcam; dilution 1:5000) was added and allowed to sit at room temperature for two hours. An ECL Western Blotting Kit was utilized in order to identify the protein bands (Amersham, Piscataway, NJ, USA).

Statistical analysis

All of the information was analyzed with GraphPad Prism 7 from GraphPad Software in San Diego, California, United States, as well as SPSS 19.0 (IBM Corp.). The statistical differences between two distinct groups were analyzed using a Student's t-test with two tails, and an analysis of variance (ANOVA) with one direction was performed on data from numerous groups. The Kaplan-Meier technique was utilized in order to draw survival curves, and the log-rank test was utilized in order to conduct statistical analysis on the gap in overall survival time that existed between the two groups. The Pearson's correlation coefficient was used to

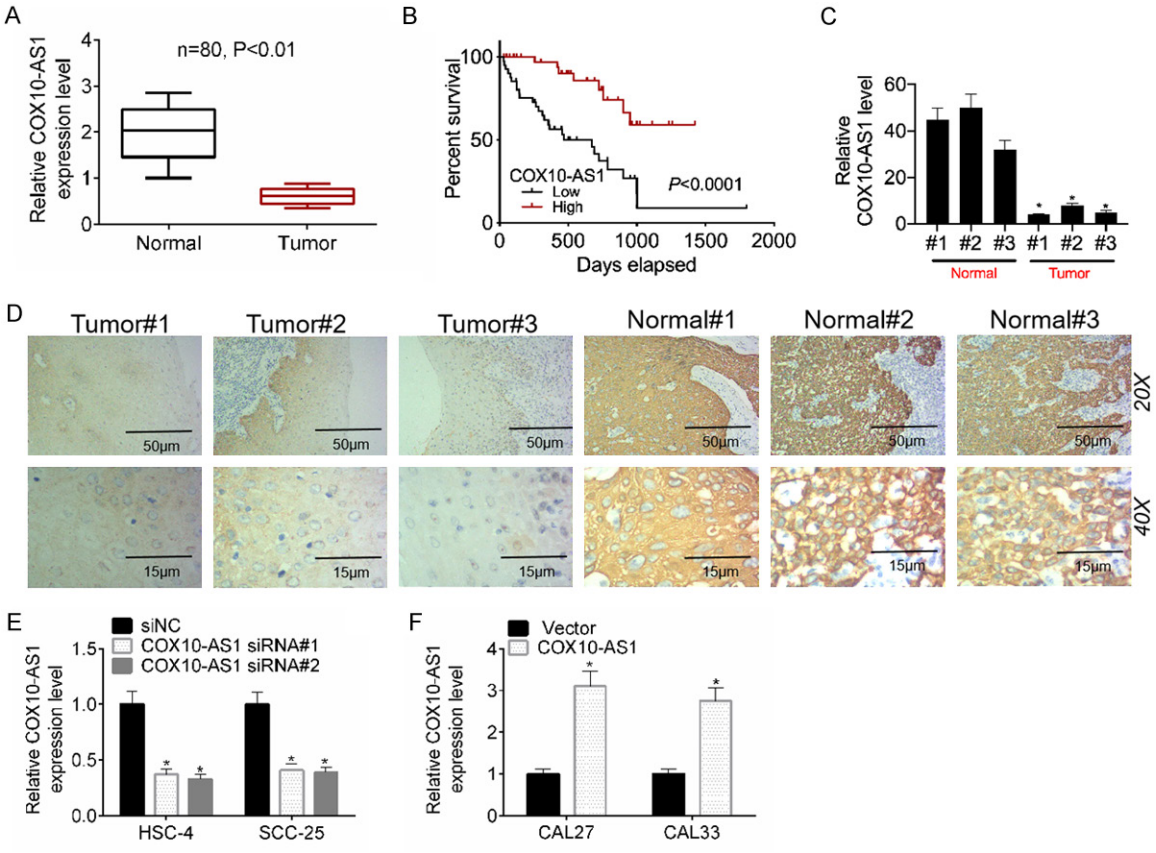

Figure 1. COX10-AS1 was repressed in OSCC and associated with a poor prognosis. A. COX10-AS1 expression in 80 OSCC tissues and normal tissues was detected by RT-PCR. B. The mean overall survival time between OSCC patients with a low expression level of COX10-AS1 and OSCC patients with a high expression level of COX10-AS1. C, D. The ISH results showed that the expression level of COX10-AS1 in OSCC tissues was significantly lower compared with the paired adjacent tissues. E and F. RT-PCR assay detected COX10-AS1 expression in OSCC cell lines. All data represent three independent experiments. Data are presented as the mean ± SD. **P*<0.05.

study the relationships between the levels of COX10-AS1 expression, miR-361-5p expression, and SPRY1 expression; between miR-361-5p expression and SPRY1 expression; and between COX10-AS1 expression and SPRY1 expression. The data were all reported using the mean together with the standard deviation, and each experiment was repeated a minimum of three times. A statistically significant difference was judged to exist if the *P* value was lower than 0.05.

Results

COX10-AS1 was repressed in OSCC and associated with a poor prognosis

RT-PCR was used to detect COX10-AS1 level in 80 cases of OSCC patients with complete clinical data and follow-up data. The relationship between COX10-AS1 expression and clinicopathological features and overall survival time was analyzed. This was done in order to verify the relationships between COX10-AS1 expression level and prognosis in OSCC patients. When compared to the similar neighboring tissues, the amount of COX10-AS1 mRNA in OSCC tumor tissues was significantly lower (**Figure 1A**). The expression of COX10-AS1 was found to have a strong correlation with both the T staging of OSCC and its regional lymph node metastases (**Table 2**). According to the results of a Kaplan-Meier survival study, patients with OSCC who had low COX10-AS1 expression had a lower chance of surviving the disease than those who had high COX10-AS1 expression (**Figure 1B**). Following this, the findings of an ISH analysis and RT-PCR assay provided further evidence that COX10-AS1 was very weakly

Table 2. The expression of COX10-AS1 and its relationship with clinicopathological features of patients with OSCC

Parameters	Total	COX10-AS1 expression		χ^2	*P* value
		Low (n = 41)	High (n = 39)		
Age				0.041	0.840
≤60	36	18	18		
>60	44	23	21		
Gender				0.050	0.823
Male	40	21	19		
Female	40	20	20		
Tumor differentiation				0.083	0.959
Well	20	10	10		
Moderate	30	16	14		
Poor	30	15	15		
T staging				26.737	0.000*
T1	19	3	16		
T2	17	4	13		
T3	36	28	8		
T4	8	6	2		
Regional lymph node metastasis				7.155	0.007*
Yes	43	28	15		
No	37	13	24		
Clinical stage				4.069	0.254
I	17	7	10		
II	23	9	14		
III	24	15	9		
IV	16	10	6		

P values reflect the relationship between COX10-AS1 expression and clinicopathological parameters with Chi-square test. P<0.05 was considered statistically significant. *P<0.05; High (COX10-AS1 expression >0.614), Low (COX10-AS1 expression ≤0.614); OSCC: Oral Squamous Cell Carcinoma.

expressed in OSCC tumor tissues and cell lines (**Figure 1C** and **1D**). Therefore, COX10-AS1 siRNA was successfully transfected in HSC-4 and SCC-25 cells to inhibit COX10-AS1 expression, and the COX10-AS1 overexpression vector was successfully transfected in CAL27 and CAL33 cells to raise COX10-AS1 expression. This was done so that COX10-AS1 expression could be increased in these cells (**Figure 1E** and **1F**).

COX10-AS1 suppressed cell migration and invasion in OSCC

The transwell results demonstrated that COX10-AS1 knockdown dramatically promoted the migration and invasion compared with the si-NC group (**Figure 2A** and **2B**). MMP-2/-9, Snail, and E-cadherin were considered as the invasion and migration-related marks [22]. COX10-AS1 knockdown inhibited the expression of MMP-2/-9 and Snail and increased E-cadherin expression (**Figure 2C**). Whereas COX10-AS1 overexpression dramatically restrained OSCC cells invasion and migration (**Figure 2D** and **2E**) and elevated the expression of MMP-2/-9 and Snail and suppressed E-cadherin expression (**Figure 2F**).

miR-361-5p was a target miRNA of COX10-AS1

Starbase V2.0 database displayed that miR-361-5p was the only target miRNA having three binding sites for COX10-AS1 (**Figure 3A**). Dual-luciferase reporter assay confirmed that miR-361-5p mimics significantly suppressed the luciferase activity of COX10-AS1 3'-UTR-wt, but miR-361-5p mimics had not affected the luciferase activity of COX10-AS1 3'-UTR-mut (**Figure 3B**). Next, COX10-AS1 silencing significantly

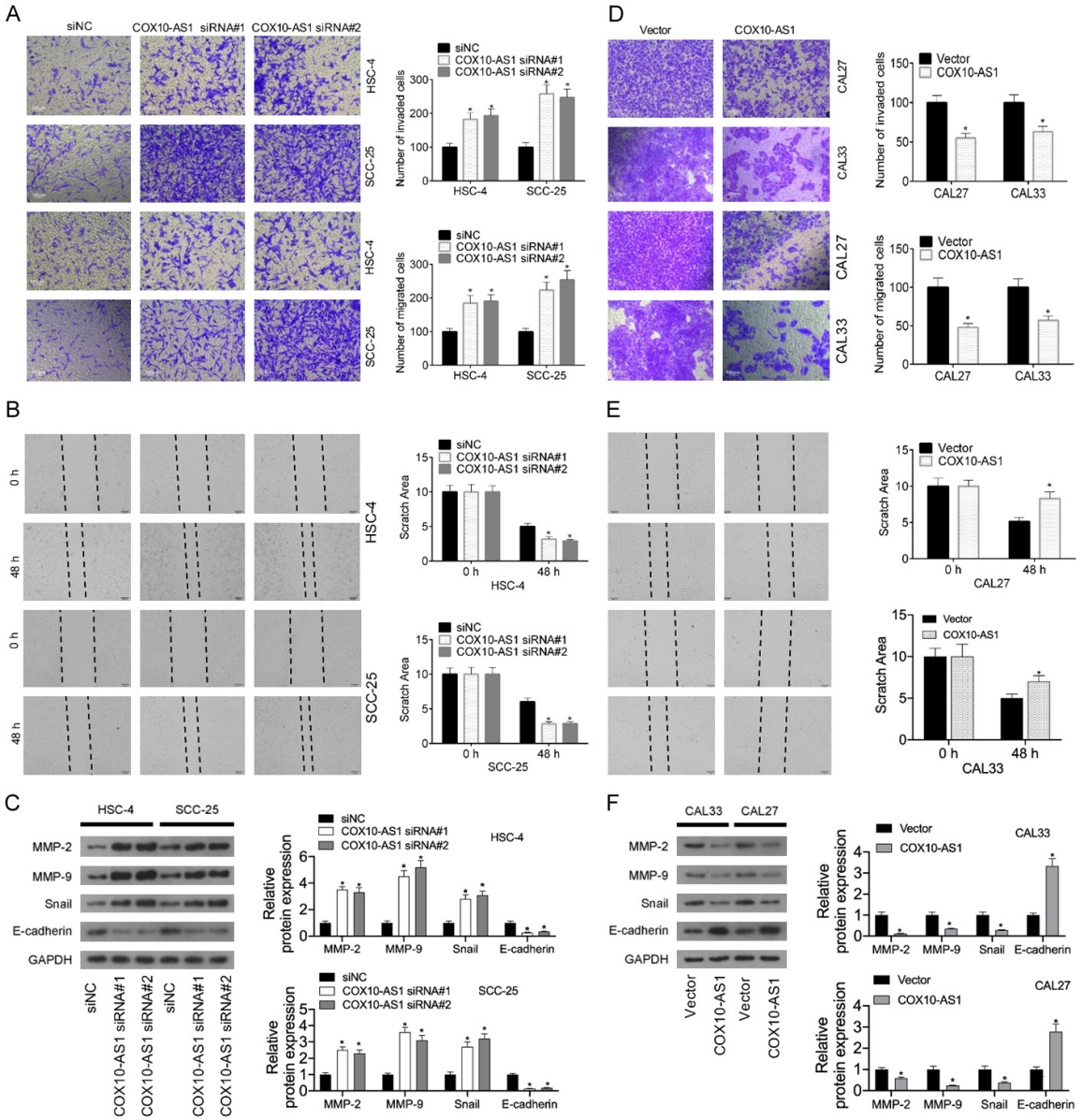

Figure 2. COX10-AS1 suppressed cell migration and invasion in OSCC. In COX10-AS1 siRNA#1/#2 transfected HSC-4 and SCC-25 cells, cell invasion (A), migration (B), and the expression of MMP-2/-9, Snail, and E-cadherin (C) were detected by transwell and western blot assays. In COX10-AS1 overexpressing vector transfected CAL27 and CAL33 cells, cell invasion (D), migration (E), and the expression of MMP-2/-9, Snail, and E-cadherin (F) were detected by transwell and western blot assays. All data represent three independent experiments. Data are presented as the mean ± SD. **P*<0.05.

improved miR-361-5p mRNA level in HSC-4 and SCC-25 cells while COX10-AS1 overexpression markedly suppressed miR-361-5p mRNA level in CAL27 and CAL33 cells (**Figure 3C**). Further, miR-361-5p expression in OSCC tumor tissues was higher compared with the corresponding adjacent tissues (**Figure 3D**) and was significantly negatively correlated with COX10-AS1 expression (**Figure 3E**). In order to further study the relationship between COX10-AS1 and miR-361-5p, we transfected CAL27 and CAL33 cells with miR-361-5p mimics or HSC-4 and SCC-25 cells with miR-361-5p inhibitors to increase and inhibit its expression, thereby for the follow-up experiments (**Figure 3F**).

COX10-AS1 regulated OSCC cell invasion and migration via miR-361-5p

Our results showed that miR-361-5p inhibitors counteracted COX10-AS1 knockdown-induced OSCC cell invasion and migration (**Figure 4A**

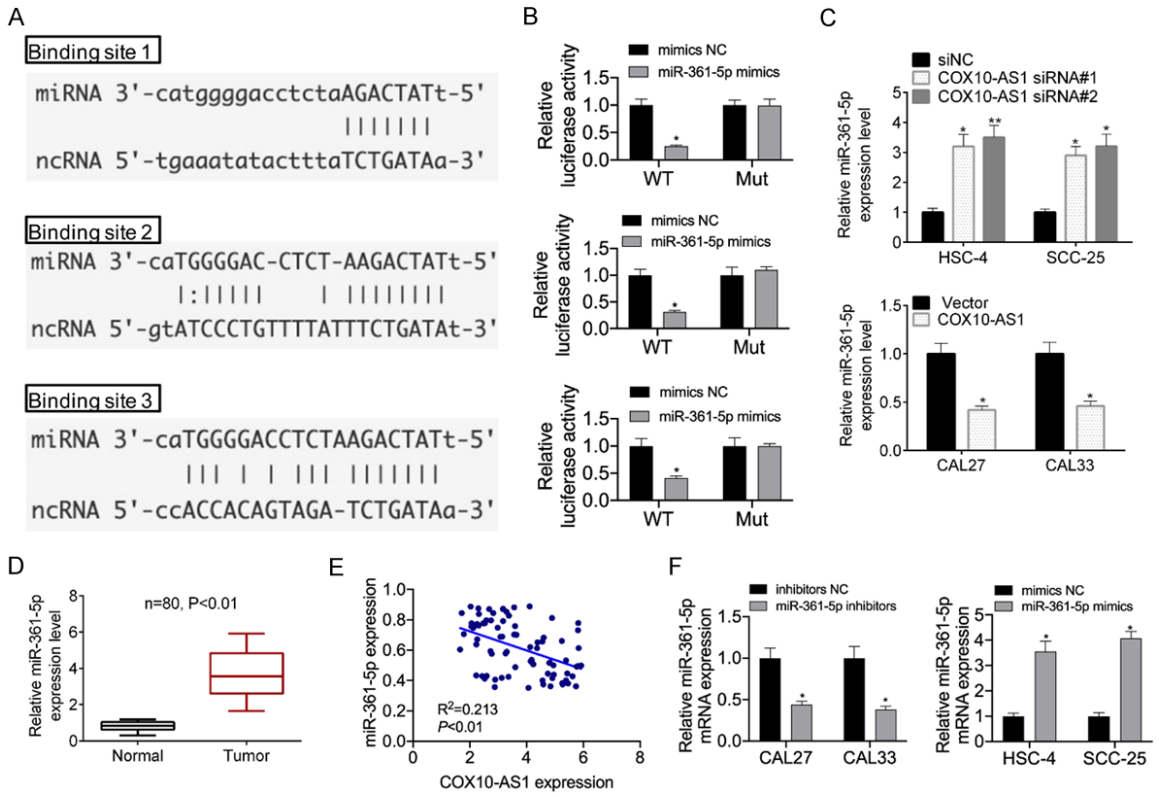

Figure 3. miR-361-5p was a target miRNA of COX10-AS1. A. A total of 3 binding sites between COX10-AS1 and miR-361-5p was shown in Starbase V2.0 database. B. Luciferase activity of COX10-AS1 (wt or mut) in miR-361-5p transfected cells was measured by a dual-luciferase reporter assay. C. miR-361-5p mRNA level were detected by RT-PCR in COX10-AS1 siRNA#1/#2 transfected HSC-4 and SCC-25 cells and COX10-AS1 overexpressing vector transfected CAL27 and CAL33 cells. D. miR-361-5p expression in 80 OSCC tissues and normal tissues was detected by RT-PCR. E. miR-361-5p expression levels are negatively correlated with COX10-AS1 expression. F. miR-361-5p mRNA level was detected by RT-PCR in miR-361-5p inhibitors transfected CAL27 and CAL33 cells and miR-361-5p mimics transfected HSC-4 and SCC-25 cells. All data represent three independent experiments. Data are presented as the mean ± SD. **P*<0.05.

and **4B**) and miR-361-5p overexpression neutralized COX10-AS1 overexpression-mediated OSCC cell invasion and migration-inhibiting (**Figure 4C** and **4D**).

SPRY1 was a target gene of miR-361-5p

TargetScan database displayed the binding site between SPRY1 and miR-361-5p (**Figure 5A**). We verified the interaction between miR-361-5p and SPRY1 in the same manner as verifying the interaction with COX10-AS1 and miR-361-5p, as evidence by miR-361-5p mimics significantly suppressing the luciferase activity of SPRY1 3'-UTR-wt, but miR-361-5p mimics had not affected the luciferase activity of SPRY1 3'-UTR-mut, and (**Figure 5B**). In addition, SPRY1 expression at the levels of mRNA and protein was inhibited by miR-361-5p mimic transfection and was elevated by miR-361-5p inhibitor transfection (**Figure 5C-F**). Subsequently, SPRY1 mRNA level in OSCC tumor tissues was lower compared with the corresponding adjacent tissues (**Figure 5G**) and was significantly negatively correlated with miR-361-5p mRNA level (**Figure 5H**). The results of IHC analysis further proved that SPRY1 was lowly expressed in OSCC tumor tissues (**Figure 5I**).

COX10-AS1 increased SPRY1 expression via sponging miR-361-5p to affect cell invasion and migration in OSCC

COX10-AS1 indicated that SPRY1 expression was positively correlated with COX10-AS1 expression (**Figure 6A**). The luciferase activity of SPRY1 wt was increased by COX10-AS1 overexpression (**Figure 6B**) and was inhibited by COX10-AS1 knockout (**Figure 6C** and **6D**). Likewise, we found in CAL27 and CAL33 cells

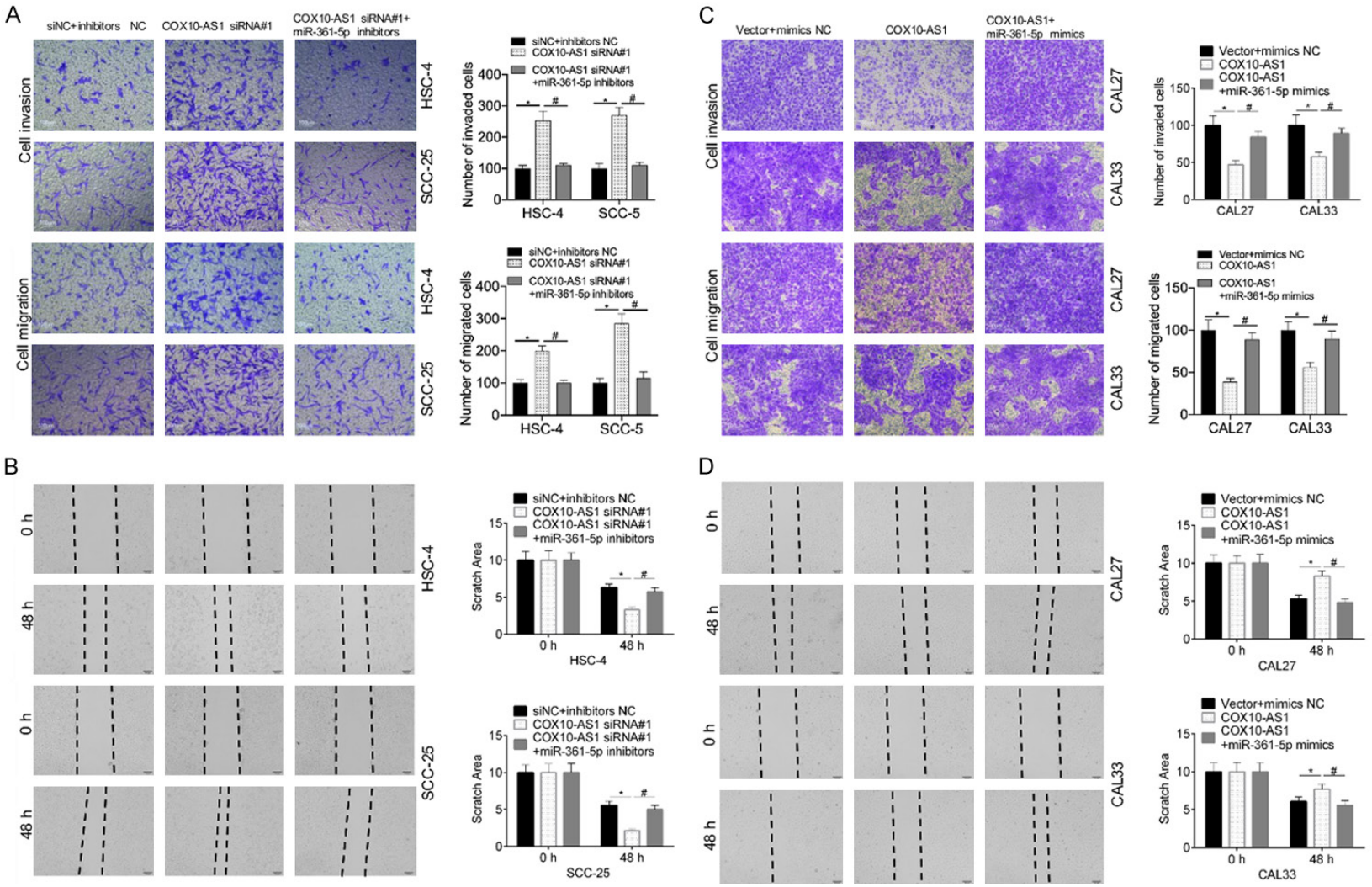

Figure 4. COX10-AS1 regulated OSCC cell invasion and migration via miR-361-5p. In COX10-AS1 siRNA#1/#2 and miR-361-5p inhibitors co-transfected HSC-4 and SCC-25 cells, cell invasion (A), and migration (B) were detected by transwell and western blot assays. In COX10-AS1 overexpressing vector and miR-361-5p mimics co-transfected CAL27 and CAL33 cells, cell invasion (C), and migration (D) were detected by transwell and western blot assays. All data represent three independent experiments. Data are presented as the mean ± SD. **P*<0.05.

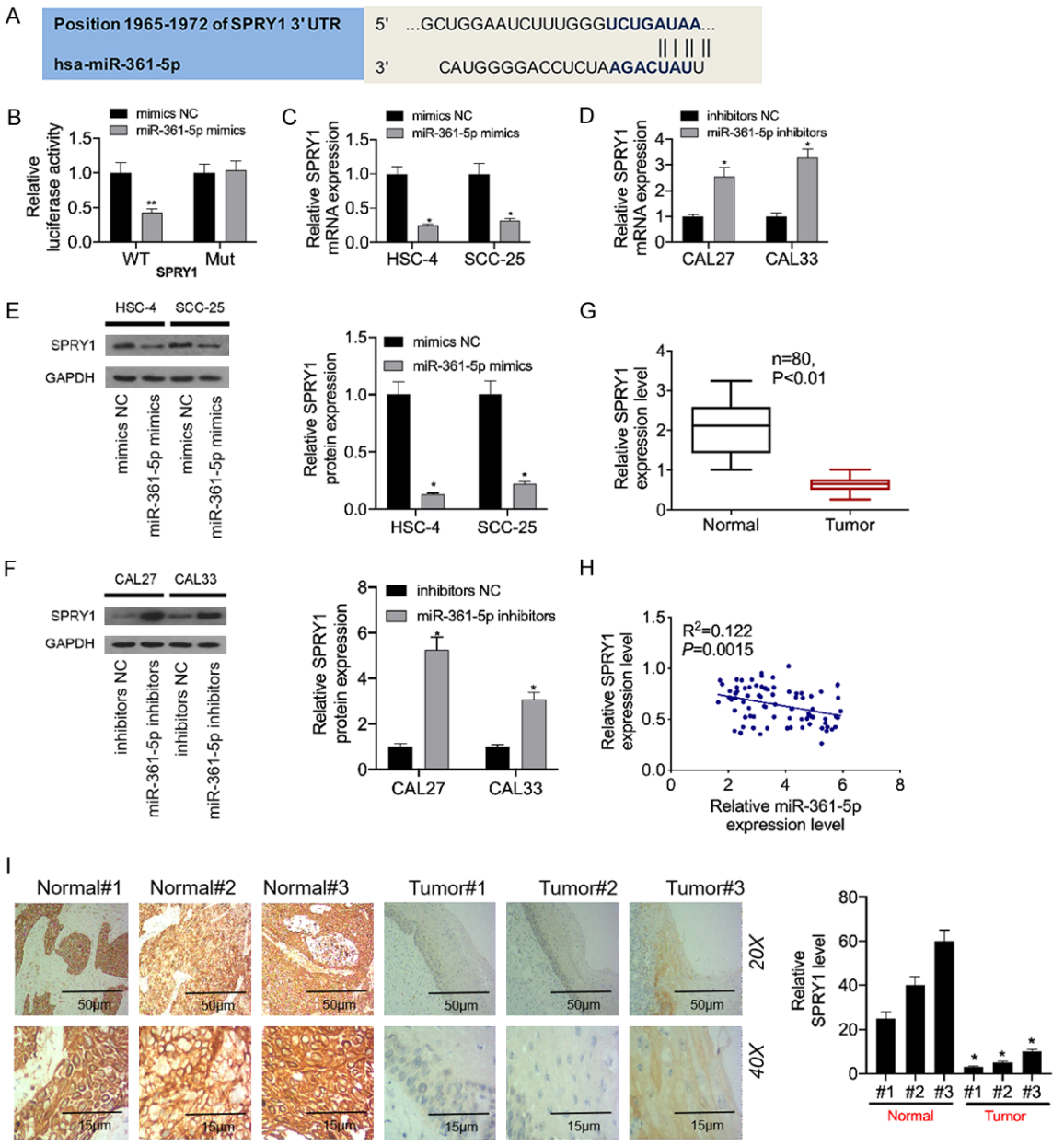

Figure 5. SPRY1 was a target gene of miR-361-5p. (A) The binding site between SPRY1 and miR-361-5p was shown in TargetScan database. (B) Luciferase activity of SPRY1 (wt or mut) in miR-361-5p transfected cells was measured by a dual-luciferase reporter assay. RT-PCR assay was used to detect SPRY1 mRNA level in miR-361-5p mimics transfected HSC-4 and SCC-25 cells (C) and miR-361-5p inhibitors transfected CAL27 and CAL33 cells (D). Western blot assay was used to detect SPRY1 protein level in miR-361-5p mimics transfected HSC-4 and SCC-25 cells (E) and miR-361-5p inhibitors transfected CAL27 and CAL33 cells (F). (G) SPRY1 expression in 80 OSCC tissues and normal tissues was detected by RT-PCR. (H) miR-361-5p expression levels are negatively correlated with SPRY1 expression. (I) The IHC results showed that the expression level of SPRY1 in OSCC tissues was significantly lower compared with the paired adjacent tissues. All data represent three independent experiments. Data are presented as the mean ± SD. **P*<0.05.

transfected with a vector expressing COX10-AS1, SPRY1 expression was increased, and in HSC-4 and SCC-25 cells transfected with COX10-AS1 knockout, SPRY1 expression was decreased (**Figure 6E** and **6F**). The immunofluorescence assay also proved that the fluorescence intensity of the SPRY1 protein in COX10-AS1-overexpression CAL27 and CAL33 cells was significantly increased, while the fluorescence intensity of the SPRY1 protein was sig-

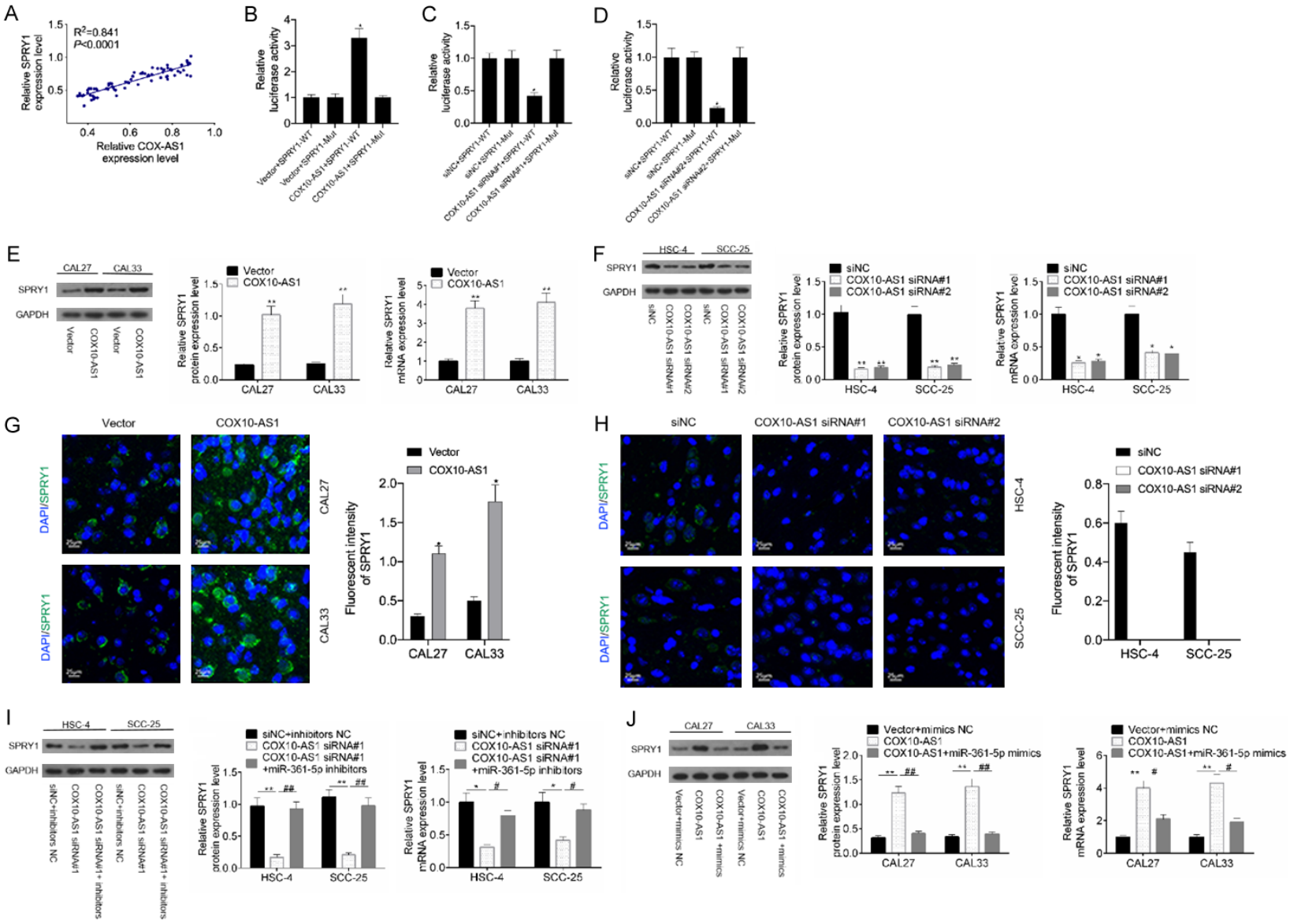

Figure 6. COX10-AS1 increased SPRY1 expression via sponging miR-361-5p. (A) COX10-AS1 expression levels are positively correlated with SPRY1 expression. Luciferase activity of SPRY1 (wt or mut) in COX10-AS1 expressing vector transfected cells (B), COX10-AS1 siRNA#1 transfected cells (C), and COX10-AS1 siRNA#2 transfected cells (D) were measured by a dual-luciferase reporter assay. RT-PCR and western blot assays were used to detected SPRY1 expression in COX10-AS1

expressing vector transfected CAL27 and CAL33 cells (E), and COX10-AS1 siRNA#1/#2 transfected HSC-4 and SCC-25 cells (F). Immunofluorescence assay was used to detect the fluorescence intensity of SPRY1 in COX10-AS1-overexpression CAL27 and CAL33 cells and (G) COX10-AS1-knockout HSC-4 and SCC-25 cells (H) (scale bars = 200 μm). In HSC-4 and SCC-25 cells co-transfected with miR-361-5p inhibitors and COX10-AS1 siRNA#1 (I) and CAL27 and CAL33 cells co-transfected with miR-361-5p mimics and COX10-AS1 expressed vector (J), RT-PCR and western blot assays were used to detected SPRY1 expression. All data represent three independent experiments. Data are presented as the mean ± SD. *P<0.05.

nificantly decreased in COX10-AS1-knockdown HSC-4 and SCC-25 cells (**Figure 6G** and **6H**). However, COX10-AS1-knockdown-mediated SPRY1 expression-inhibiting was reversed by miR-361-5p inhibitors and COX10-AS1-overexpression-mediated SPRY1 expression-increasing was abolished by miR-361-5p mimics (**Figure 6I** and **6J**).

In SPRY1-overexpressing HSC-4 cells (**Figure 7A**), the results of functional experiments show that COX10-AS1-knockdown-mediated cell invasion and migration-promotion (**Figure 7B** and **7C**), MMP-2/-9 and Snail expression-increase, and E-cadherin expression-inhibition (**Figure 7D**) was reversed by SPRY1-overexpression. Then, in SPRY1-knockdown CAL33 cells (**Figure 7E**), COX10-AS1 overexpression-mediated cell invasion and migration-suppression (**Figure 7F** and **7G**), MMP-2/-9 and Snail expression-inhibition, and E-cadherin expression-increase (**Figure 7H**).

Discussion

It has been stated that the essential elements that allow tumor metastasis are those that increase the migratory and invasive capabilities of tumor cells [23]. Invasion of cancer cells into local tissues and metastasis of cancer cells to distant areas are two distinct but linked processes. Cancer cells can invade local tissues and metastasize to distant locations. When cancer cells make their way into the tissues of the host, an invasion has occurred. Tissue invasion refers to the process by which tumor cells expand into the surrounding environment and become more prevalent. This can happen at any stage of the disease. The process of tumor cells detaching from the primary tumor, migrating to a new location, and creating a new or secondary tumor in a new environment is referred to as metastasis. This process takes place in a new environment. Both the invasion and migration of tumor cells are intricate processes that are made easier by preexisting biological systems. These previous biological systems are employed by both of these complicated processes. Notably, around one-third of individuals diagnosed with OSCC may develop metastases [24]. When it comes to the migration and invasion of OSCC cells, LncRNAs are an absolutely necessary component. Through the promotion of epithelial-mesenchymal transition, agents such as HOTAIR, LINC00284, and HOXA11-AS contributed to the progression of OSCC metastases (EMT) [25-27]. MMP-2 and MMP-9 are two members of the zinc-dependent endopeptidase family that are responsible for the degradation of extracellular matrix. Both of these enzymes are highly up-regulated in cancerous tissues in order to facilitate the migration and invasion of tumor cells [28]. Snail and E-cadherin have both been investigated as potential biomarkers for a variety of different metastases caused by tumors [29]. In light of this, we decided to employ the aforementioned four proteins as markers representing OSCC cell migration and invasion for the purpose of this investigation. Because of their vast variety of activities and numerous unknown capabilities, lncRNAs account for a considerable fraction of human ncRNAs. Numerous studies in recent years have found that dysregulation of lncRNA expression is directly associated to the development and prognosis of several illnesses, particularly malignant tumors. Currently, there are three basic functional concepts for lncRNA: (1) it is a functional biological molecule that can interact with DNA, proteins, and other RNAs in cells; (2) gene regulatory elements are embedded in the transcriptional bodies of lncRNA genes, and the activity of lncRNA genes directly affects the activity of regulatory elements; and (3) it affects the genome's transcriptional process, thus influencing gene activity. lncRNAs can perform one or more of these activities concurrently, and it is because of these functionalities that lncRNAs are able to operate as they do. These capabilities allow lncRNAs to control gene expression as RNAs at the pre-, transcriptional, and post-transcriptional levels, and they play an important role in the genesis and progression of many malignancies. As a result, lncRNAs have the potential to be used as a diagnostic

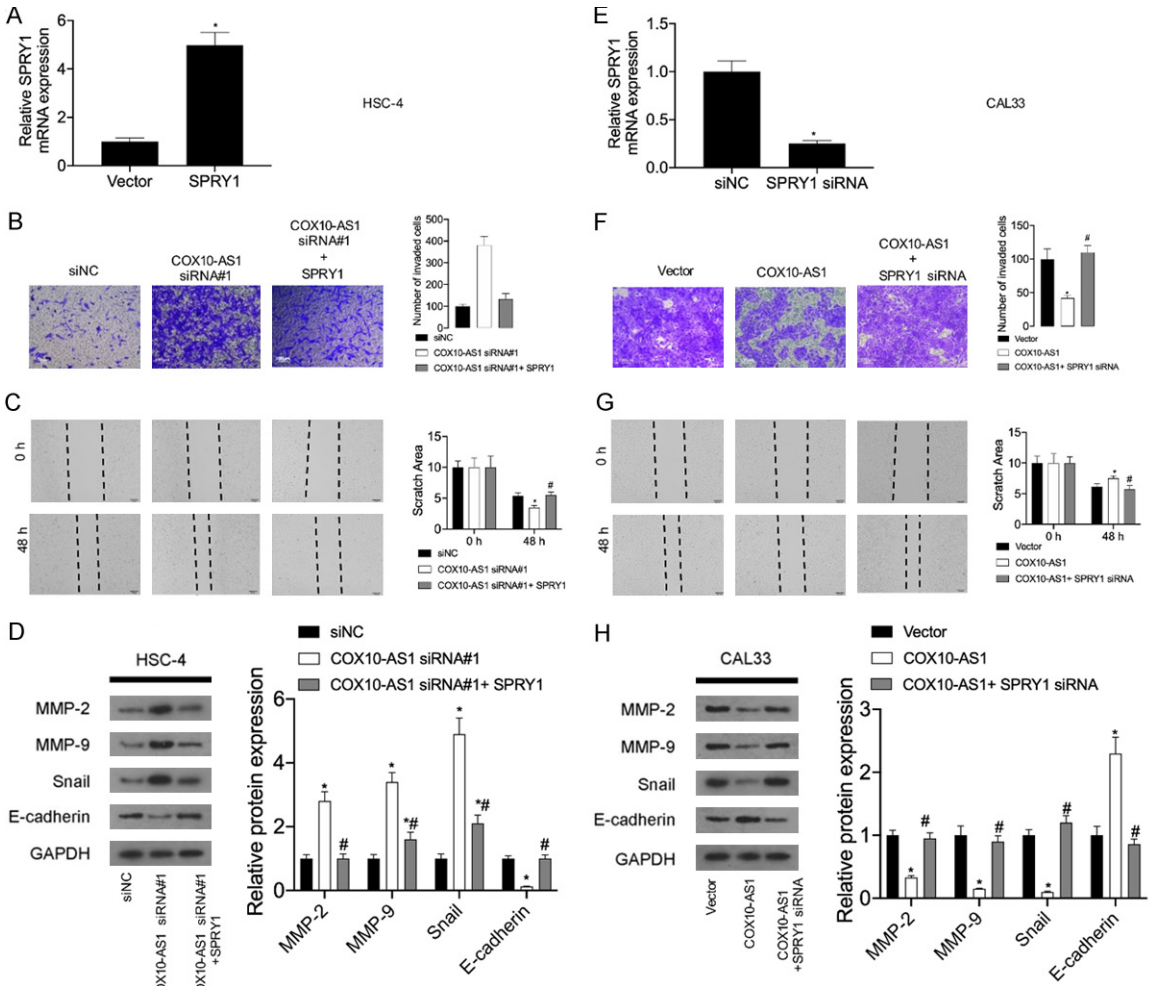

Figure 7. COX10-AS1 affect cell invasion and migration, and the related gene expression via SPRY1 in OSCC. (A) RT-PCR analysis of SPRY1 mRNA level in SPRY1-overexpression HSC-4 cells. Transwell, Scratch-Wound, and western blot assays were used to detect cell invasion (B), migration (C), and the expression of MMP-2/-9, Snail, and E-cadherin (D) in HSC-4 cells co-transfected with COX10-AS1 siRNA#1 and SPRY1 expressed vector. (E) RT-PCR analysis of SPRY1 mRNA level in SPRY1-knockout CAL33 cells. Transwell, Scratch-Wound, and western blot assays were used to detect cell invasion (F), migration (G), and the expression of MMP-2/-9, Snail, and E-cadherin (H) in HSC-4 cells co-transfected with SPRY1 siRNA and COX10-AS1 expressed vector. All data represent three independent experiments. Data are presented as the mean ± SD. *P<0.05.

and prognostic biomarker as well as a therapeutic targets in malignant tumors. COX10-AS1 was found to be reduced in OSCC patients in a study, and its overexpression was found to suppress cell invasion and migration, as well as increase the expression of MMP-2/-9 and Snail and inhibit the expression of E-cadherin, whereas its inhibition was found to promote cell invasion and migration and reduce the expression of MMP-2/-9 and Snail and increase the expression of E-cadherin, which indicates that COX10-AS1 may exert inhibitory influences. In the meanwhile, prognosis is not good for OSCC patients who have low expression of COX10-AS1. According to the findings presented above, a low level of COX10-AS1 expression is indicative of an oncogene that contributes to OSCC metastasis. Because of this, more research on the mechanism of COX10-AS1 in OSCC is required.

It was shown that miR-361-5p was not only a target miRNA of COX10-AS1, but that COX10-AS1 also sponged miR-361-5p in glioblastomas [16]. We discovered that there are three binding sites between COX10-AS1 and miR-361-5p, which is evidence that the two molecules have a robust contact history with one another. Based on the results of previous studies, we found that miR-361-5p overexpression inhibits

cell proliferation and metastasis in cervical cancer [30] and glioma [16], but it plays a pro-cancer role in bile duct cancer [31], proving miR-361-5p could be either an anti-cancer factor or an anti-cancer factor in different cancers. miR-361-5p was highly expressed in aggressive oral carcinoma [32]. However, there has been no investigation into the function of miR-361-5p in OSCC. In the research that we conducted, the effects of COX10-AS1 deletion on the promotion of cell invasion and migration in OSCC were counteracted by miR-361-5p mimics. Therefore, we have a strong suspicion that the various functions of miRNA-361-5p in various malignancies are attributable to the various functions of the upstream lncRNA that suppresses its production as well as the various functions of the downstream target genes that are controlled by it in tumors.

One of the members of the sprouty family, sprouty receptor tyrosine kinase (RTK) signaling antagonist 1 (SPRY1), was identified as one of the target genes for the microRNA known as miR-361-5p [33]. In a number of the developmental and physiological processes, sprouty proteins act as antagonists of the RTK signaling pathway. According to the findings of numerous research studies, sprouty proteins may both negatively and favorably affect RTK-induced signaling pathways by utilizing a variety of methods, therefore integrating a wide range of biological activities into a single molecule [34]. In gastric cancer, psoriasis, and systemic lupus erythematosus, SPRY1 has been examined as a candidate for playing a significant role in the regulation of cell proliferation and migration [35, 36]. In addition, SPRY1 was reported to be lowly expressed in gliomas to promote cell proliferation [16]. We observed in this study that SPRY1 had a very low level of expression in the tumor tissues of OSCC patients. After that, COX10-AS1 soaked up miR-361-5p to limit SPRY1 expression, and the effects of COX10-AS1 knockout on cell invasion and migration were counteracted by overexpressing SPRY1. The aforementioned research, together with our own findings, provided indirect evidence that SPRY1 acts as a tumor suppressor in OSCC, and that inhibiting its activity might lead to increased OSCC metastasis.

Our research on the mechanistic elements, however, is focused on *in vitro* cell models. Therefore, further *in vivo* investigation of this data would be necessary. The new focus of our upcoming study will be on whether COX10-AS1, a crucial element in promoting OSCC, has the potential to develop into a target of OSCC.

Conclusion

Low expression of COX10-AS1 was identified in OSCC tumor tissues and was significantly related to a poor prognosis. SPRY1, as a target gene of miR-361-5p, is lowly expressed in OSCC patients, and was negatively regulated by miR-361-5p and positively regulated by COX10-AS1. Downregulation of COX10-AS1 promoted OSCC cell invasion and migration via sponging miR-361-5p to inhibit SPRY1 expression, indicating COX10-AS1-miR-361-5p-SPRY1 regulatory network is a putative target for OSCC treatment.

Disclosure of conflict of interest

None.

Address correspondence to: Jing Deng, Department of Otolaryngology, Hospital of Chengdu University of Traditional Chinese Medicine, No. 39, Twelve Bridges Road, Chengdu 610075, Sichuan, China. Tel: +86-028-87783481; Fax: +86-028-87783481; E-mail: 38225207@qq.com

References

[1] Panarese I, Aquino G, Ronchi A, Longo F, Montella M, Cozzolino I, Roccuzzo G, Colella G, Caraglia M and Franco R. Oral and oropharyngeal squamous cell carcinoma: prognostic and predictive parameters in the etiopathogenetic route. Expert Rev Anticancer Ther 2019; 19: 105-119.

[2] Chen W, Zheng R, Baade PD, Zhang S, Zeng H, Bray F, Jemal A, Yu XQ and He J. Cancer statistics in China, 2015. CA Cancer J Clin 2016; 66: 115-132.

[3] Feng RM, Zong YN, Cao SM and Xu RH. Current cancer situation in China: good or bad news from the 2018 global cancer statistics? Cancer Commun (Lond) 2019; 39: 22.

[4] Hayes RB, Ahn J, Fan X, Peters BA, Ma Y, Yang L, Agalliu I, Burk RD, Ganly I, Purdue MP, Freedman ND, Gapstur SM and Pei Z. Association of oral microbiome with risk for incident head and neck squamous cell cancer. JAMA Oncol 2018; 4: 358-365.

[5] Dykes IM and Emanueli C. Transcriptional and post-transcriptional gene regulation by long non-coding RNA. Genomics Proteomics Bioinformatics 2017; 15: 177-186.

[6] Yuan SJ, Li SY, Wang YH, Zhang HF, Hua Y and Wang T. The clinical significance, prognostic value and biological role of lncRNA LINC01793 in oral squamous cell carcinoma. Arch Oral Biol 2021; 125: 105105.
[7] Li J, Xu X, Zhang D, Lv H and Lei X. LncRNA LHFPL3-AS1 promotes oral squamous cell carcinoma growth and cisplatin resistance through targeting miR-362-5p/CHSY1 pathway. Onco Targets Ther 2021; 14: 2293-2300.
[8] Lv T, Liu H, Wu Y and Huang W. Knockdown of lncRNA DLEU1 inhibits the tumorigenesis of oral squamous cell carcinoma via regulation of miR-149-5p/CDK6 axis. Mol Med Rep 2021; 23: 447.
[9] Wang X, Guo Y, Wang C, Wang Q and Yan G. Long noncoding RNA ZEB1-AS1 downregulates miR-23a, promotes tumor progression, and predicts the survival of oral squamous cell carcinoma patients. Onco Targets Ther 2021; 14: 2699-2710.
[10] Gao P, Sun D, Guo H, Wu Z and Chen J. LncRNA CCAT2 promotes proliferation and suppresses apoptosis of colorectal cancer cells. J BUON 2020; 25: 1840-1846.
[11] Yan L, Wu X, Yin X, Du F, Liu Y and Ding X. LncRNA CCAT2 promoted osteosarcoma cell proliferation and invasion. J Cell Mol Med 2018; 22: 2592-2599.
[12] Sun SL, Shu YG and Tao MY. LncRNA CCAT2 promotes angiogenesis in glioma through activation of VEGFA signalling by sponging miR-424. Mol Cell Biochem 2020; 468: 69-82.
[13] Marin-Bejar O, Mas AM, Gonzalez J, Martinez D, Athie A, Morales X, Galduroz M, Raimondi I, Grossi E, Guo S, Rouzaut A, Ulitsky I and Huarte M. The human lncRNA LINC-PINT inhibits tumor cell invasion through a highly conserved sequence element. Genome Biol 2017; 18: 202.
[14] Lan X, Sun W, Dong W, Wang Z, Zhang T, He L and Zhang H. Downregulation of long noncoding RNA H19 contributes to the proliferation and migration of papillary thyroid carcinoma. Gene 2018; 646: 98-105.
[15] Li XX, Wang LJ, Hou J, Liu HY, Wang R, Wang C and Xie WH. Identification of long noncoding RNAs as predictors of survival in triple-negative breast cancer based on network analysis. Biomed Res Int 2020; 2020: 8970340.
[16] Zhou C, Jiang X, Liang A, Zhu R, Yang Y, Zhong L and Wan D. COX10-AS1 facilitates cell proliferation and inhibits cell apoptosis in glioblastoma cells at post-transcription level. Neurochem Res 2020; 45: 2196-2203.
[17] Feng L, Houck JR, Lohavanichbutr P and Chen C. Transcriptome analysis reveals differentially expressed lncRNAs between oral squamous cell carcinoma and healthy oral mucosa. Oncotarget 2017; 8: 31521-31531.
[18] Fabian MR, Sonenberg N and Filipowicz W. Regulation of mRNA translation and stability by microRNAs. Annu Rev Biochem 2010; 79: 351-379.
[19] Paraskevopoulou MD and Hatzigeorgiou AG. Analyzing MiRNA-LncRNA interactions. Methods Mol Biol 2016; 1402: 271-286.
[20] Chen L, Zhou Y and Li H. LncRNA, miRNA and lncRNA-miRNA interaction in viral infection. Virus Res 2018; 257: 25-32.
[21] Wang W, Lou W, Ding B, Yang B, Lu H, Kong Q and Fan W. A novel mRNA-miRNA-lncRNA competing endogenous RNA triple sub-network associated with prognosis of pancreatic cancer. Aging (Albany NY) 2019; 11: 2610-2627.
[22] Liu D, Han Y, Liu L, Ren X, Zhang H, Fan S, Qin T and Li L. Parthenolide inhibits the tumor characteristics of renal cell carcinoma. Int J Oncol 2021; 58: 100-110.
[23] Trepat X, Chen Z and Jacobson K. Cell migration. Compr Physiol 2012; 2: 2369-2392.
[24] Zanoni DK, Montero PH, Migliacci JC, Shah JP, Wong RJ, Ganly I and Patel SG. Survival outcomes after treatment of cancer of the oral cavity (1985-2015). Oral Oncol 2019; 90: 115-121.
[25] Niu X, Yang B, Liu F and Fang Q. LncRNA HOXA11-AS promotes OSCC progression by sponging miR-98-5p to upregulate YBX2 expression. Biomed Pharmacother 2020; 121: 109623.
[26] Wu Y, Zhang L, Zhang L, Wang Y, Li H, Ren X, Wei F, Yu W, Liu T, Wang X, Zhou X, Yu J and Hao X. Long non-coding RNA HOTAIR promotes tumor cell invasion and metastasis by recruiting EZH2 and repressing E-cadherin in oral squamous cell carcinoma. Int J Oncol 2015; 46: 2586-2594.
[27] Yan D, Wu F, Peng C and Wang M. Silencing of LINC00284 inhibits cell proliferation and migration in oral squamous cell carcinoma by the miR-211-3p/MAFG axis and FUS/KAZN axis. Cancer Biol Ther 2021; 22: 149-163.
[28] Timokhina E, Strizhakov A, Ibragimova S, Gitel E, Ignatko I, Belousova V and Zafiridi N. Matrix metalloproteinases MMP-2 and MMP-9 occupy a new role in severe preeclampsia. J Pregnancy 2020; 2020: 8369645.
[29] Tavakolian S, Goudarzi H and Faghihloo E. E-cadherin, Snail, ZEB-1, DNMT1, DNMT3A and DNMT3B expression in normal and breast cancer tissues. Acta Biochim Pol 2019; 66: 409-414.
[30] Wu X, Xi X, Yan Q, Zhang Z, Cai B, Lu W and Wan X. MicroRNA-361-5p facilitates cervical cancer progression through mediation of epithelial-to-mesenchymal transition. Med Oncol 2013; 30: 751.
[31] Lu WX. Long non-coding RNA MEG3 represses cholangiocarcinoma by regulating miR-361-

5p/TRAF3 axis. Eur Rev Med Pharmacol Sci 2019; 23: 7356-7368.
[32] Hilly O, Pillar N, Stern S, Strenov Y, Bachar G, Shomron N and Shpitzer T. Distinctive pattern of let-7 family microRNAs in aggressive carcinoma of the oral tongue in young patients. Oncol Lett 2016; 12: 1729-1736.
[33] Chen QY, Li YN, Wang XY, Zhang X, Hu Y, Li L, Suo DQ, Ni K, Li Z, Zhan JR, Zeng TT, Zhu YH, Li Y, Ma LJ and Guan XY. Tumor fibroblast-derived FGF2 regulates expression of SPRY1 in esophageal tumor-infiltrating T cells and plays a role in T-cell exhaustion. Cancer Res 2020; 80: 5583-5596.
[34] Christofori G. Split personalities: the agonistic antagonist sprouty. Nat Cell Biol 2003; 5: 377-379.
[35] He X, Wang J, Chen J, Han L, Lu X, Miao D, Yin D, Geng Q and Zhang E. lncRNA UCA1 predicts a poor prognosis and regulates cell proliferation and migration by repressing p21 and SPRY1 expression in GC. Mol Ther Nucleic Acids 2019; 18: 605-616.
[36] Stepicheva NA and Song JL. Function and regulation of microRNA-31 in development and disease. Mol Reprod Dev 2016; 83: 654-674.